Propylene polymerization with a bisiminepyridine iron complex: activation with Ph$_3$C [B(C$_6$F$_5$)$_4$] and AlR$_3$; iron hydride species in the catalytic cycle

Sebastian Thomas Babik, Gerhard Fink*

Max-Planck-Institut für Kohlenforschung, Kaiser-Wilhelm-Platz 1, 45470 Mülheim an der Ruhr, Germany

Abstract

In this work, the complex 2,6-bis [1-(2-isopropyl-6-methylphenylimino)ethyl]-pyridineiron(II)dichloride was used for propylene polymerization. Activation with Ph$_3$C [B(C$_6$F$_5$)$_4$] and subsequent treatment with triisobutylaluminium or triethylaluminium generated a very active polymerization catalyst for propylene. The kinetics of this polymerization reaction were investigated with mass-flowmeters. Further we show propagation-time-profiles of this reaction. Depending on the nature of the aluminiumalkyl we are able to determine different aliphatic endgroups in the polymer using ^{13}C NMR spectroscopy. Addition of hydrogen to the polymerization leads to higher activities and allows us to formulate a complete catalytic reaction cycle containing an iron hydride species. This cycle comprises one starting cycle and two propagation cycles which can be controlled with the aluminiumtrialkyl-propylene ratio.
© 2002 Elsevier Science B.V. All rights reserved.

Keywords: Bisiminepyridine iron complex; Propylene polymerization; Propagation-time-profiles; Aluminiumtrialkyls; Iron hydride species

1. Introduction

For some years now, there has been a great academic [1–9] and industrial [10–13] interest in polymerization catalysts based on several imine complexes of late transition metals such as cobalt, iron, nickel or palladium. These kinds of catalysts are easier to synthesise and more tolerant to polar groups than metallocenes. Based on the works of Small and Brookhart [5], in which propylene was polymerized with bisiminepyridine iron complexes, we investigated the kinetics and mechanism of propylene polymerization. First of all, it was necessary to increase the catalyst activity for the propylene polymerization, because activation with MAO (methylaluminoxan) used by Brookhart yields an unsatisfactory amount of polymer. Activation of the bisiminepyridine iron complex with Ph$_3$C [B(C$_6$F$_5$)$_4$] and subsequent treatment with TIBA produces very high maximum activities exceeding 1100 kg PP/mol Fe h bar [C$_3$H$_6$]. With different aluminiumtrialkyls the nature of the active iron alkyl species that starts the polymerization can be varied and the relevant aliphatic endgroups can be detected by ^{13}C NMR spectroscopy. Addition of 8 vol.% hydrogen to the polymerization leads once more to higher activities and implies the presence of an iron hydride species in the catalytic cycle. With our results we can propose a complete catalytic cycle consisting of two propagation cycles and one starting cycle.

* Corresponding author. Tel.: +49-208-306-2240;
fax: +49-208-306-2980.
E-mail address: fink@mpi-muelheim.mpg.de (G. Fink).

2. Experimental part

2.1. General considerations

The handling of water- and air-sensitive compounds was performed under an argon atmosphere using Schlenk techniques.

2.2. Materials

Methanol was dried over CaH_2/Mg and distilled. Toluene was distilled from sodium. THF was distilled from MgH_2. 2,6-Diacetylpyridine, 2-isopropyl-6-methylaniline, 97% formic acid and $FeCl_2$ were purchased from Aldrich and used without further purification. MAO (10 wt.% solution in toluene) and Ph_3C [$B(C_6F_5)_4$] were purchased from Witco. Triisobutylaluminium (TIBA) and triethylaluminium (TEA) were produced in our institute's facility. Propylene (99.5%) was purchased from Messer-Griesheim and purified by passage through columns of molecular sieves (3 Å) and $NaAlEt_4$.

2.3. Synthesis of 2,6-bis [1-(2-isopropy-6-methylphenylimino)ethyl]-pyridine (L)

2,6-Diacetylpyridine (1.14 g, 7 mmol) was dissolved in 15 ml of dry methanol in a 50 ml round-bottom flask equipped with a condenser. 2-Isopropyl-6-methylaniline (6.27 g, 42 mmol) was added at 45 °C via a dropping funnel. Four drops of 97% formic acid were added and the clear, brown solution was allowed to stir in the sealed flask at 60 °C for 1 h. After stirring overnight at room temperature the resultant pale yellow solid precipitate, was collected by filtration, washed with cold methanol and dried. The yield was 2.44 g (82%) of pure ligand.

^{1}H NMR ($CDCl_3$): $\delta = 8.43$–8.41 (d, 2, py-H_m); 7.89–7.84 (t, 1, py-H_p); 7.13–7.10 (m, 2, H_{aryl}); 7.02–6.96 (m, 4, H_{aryl}); 2.79–2.74 (septet, 2, $CHMe_3$); 2.19 (s, 6, N = CCH_3); 1.97 (s, 6, $ArCH_3$); 1.15–1.13 (d, 6, $CHCH_3$); 1.09–1.07 ppm (d, 6, $CHCH_3$, $^3J_{H,H(i\text{-pr})} = 6.93$ Hz). IR (KBr): 3068 (m, H–C=), 2963–2868 (s, H–C), 1640 cm^{-1} (vs, C=N).

2.4. Synthesis of the iron complex

Dry $FeCl_2$ (700 mg; 5.5 mmol) in 20 ml dry THF was stirred under an argon atmosphere in a 100 ml flame-dried two-neck-flask. A solution of ligand L (2.4 g; 5.7 mmol), in 25 ml dry THF was added slowly at room temperature via a dropping funnel. The brown suspension of $FeCl_2$ turned into a immediately to a blue colour. The mixture was then stirred under argon for one additional hour. Then pentane was added to the blue suspension and the solid was filtered and dried under argon. The light-blue complex was isolated in near quantitative yield.

$C_{29}H_{35}N_3FeCl_2$ (552.37): calcd. C, 63.06; H, 6.39; N, 7.61. Found C, 62.89; H, 6.45; N, 7.56. MS (70 eV): $m/z = 551$ (M^+), 516 (M^+–Cl), 425 (M^+–$FeCl_2$ = $Ligand^+$), 410 (100%, L^+–Me).

2.5. Polymerization procedure

The polymerizations were carried out in a 250 ml glass autoclave (Büchi AG, Uster/CH) with a mechanical stirrer (1200 rpm) under constant propylene pressure of 2 bar and constant temperature. To guarantee inert reaction conditions the autoclave was evacuated and back-filled with argon three times. Then the reactor was filled with toluene and the aluminiumtrialkyl, thermostated and saturated with propylene (total volume of the liquid phase: 120 ml). After saturation, the iron complex and the borate were added in the reactor via an injection system with an excess pressure of argon or, in case of the experiments with hydrogen, with an excess pressure of hydrogen. The consumption of propylene was continuously detected with Brooks mass-flowmeters (Brooks Instruments B.V.). To stop the polymerization the excess pressure of propylene was vented and methanol was added to the reactor. The reaction mixture was poured into 600 ml of a diluted solution of hydrochloric acid in methanol and stirred overnight. The precipitated polymer was filtered, washed with fresh methanol and dried at 50 °C in a vacuum oven.

2.6. Polymer characterization

The microstructure of the polymers was analysed with ^{13}C NMR spectroscopy. The polymer (159 mg) was dissolved in 3 ml of 1,2,4-trichlorobezene/1,1,2,2-tetrachloroethane–d_2 (volume ratio, 2.5/1) in a 10 mm NMR tube and measured with proton broad-band decoupling at 120 °C on a Bruker AMX 300 spectrometer at 75.5 MHz. The molar mass experiments

were carried out in 1,2,4-trichlorobezene at 155 °C using gel permeation chromatography (Waters) 150-C with a viscosity detector (Viscotek) and a LC 300 Transform (Lab Connections). GPC data were obtained using a calibration file which was performed with narrow polystyrene and polyethylene standards.

3. Results and discussion

3.1. Activation with MAO

Using the methodology described in Section 2, propylene was polymerized with the iron complex (Fig. 1) using MAO as co-catalyst. Under the given conditions (Table 1) we always observed low activities and obtained wax-like polymers. The isotacticity index was about 65% in all cases and independent of the Al/Fe ratio.

The tacticity of the obtained polymers was determined with ^{13}C NMR spectra focusing on the region of the methylpentads between 22.0 and 19.5 ppm. The pentad distribution is shown in Table 2.

It was possible to determine the nature of the aliphatic endgroups in the polymer using the ^{13}C NMR
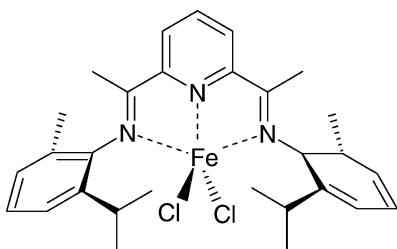

Fig. 1. Structure of the used iron complex: 2,6-bis [1-(2-isopropyl-6-methylphenylimino)ethyl]-pyridineiron(II)dichloride.

Table 1
Propylene produced by MAO activation[a]

Al/Fe-ratio	Activity (kg PP/mol Fe h)	Isotacticity %-mmmm pentad	M_n	M_w/M_n
60:1	14	65	3500	1.30
80:1	19	65	3300	1.35
100:1	11	62	3700	1.30
150:1	7	64	3800	1.26

[a] Conditions: [Fe] $= 2.6 \times 10^{-5}$ mol; $p = 1.9$ bar propylene pressure; TP $= 25$ °C; duration of polymerization: 1 h; solvent: toluene.

Table 2
Pentadanalysis of polypropylene produced by MAO activation[a]

Pentad	mmmm	mmmr	mmrr	mrmm/rrmr	mrmr	mrrm
%	65	14.3	3.9	12.9	2.8	1.1

[a] Conditions: [Fe] $= 2.6 \times 10^{-5}$ mol; $p = 1.9$ bar propylene pressure; TP $= 25$ °C, duration of polymerization: 1 h; solvent: toluene; [Al]/[Fe]-ratio $= 80 : 1$.

spectroscopy. In the region between 45 and 10 ppm significant signals arising from endgroups are found. With the MAO activated polymerization only detectable aliphatic endgroups are n-butyl groups. We explain later how n-butyl endgroups are formed during the polymerization.

3.2. Activation with Ph$_3$C [B(C$_6$F$_5$)$_4$] and subsequent treatment with aluminiumtrialkyls[14,15]

Due to the low activity of MAO as co-catalyst we investigated alternative methods to activate the iron complex. It is well known, that metallocenedialkyls can be activated with boranes or borates. Because dialkyl complexes of iron are not known, we chose a different route. Treatment of the dichloride of the iron complex (Scheme 1) with Ph$_3$C [B(C$_6$F$_5$)$_4$] followed by TIBA generates a high concentration of active species for the propylene polymerization.

Step 1. The formation of the predicted triphenylmethylchloride was confirmed by coupled HPLC/UV–Vis spectroscopy. With the addition of 80 equiv. TIBA (Scheme 2) the second chloride is substituted by an isobutyl group and an iron–carbon bond that can insert propylene is generated.

Step 2. With this activation procedure we achieved activities of about 1100 kg PP/mol Fe h bar [C$_3$H$_6$] which is more than 200 times higher than with MAO activation. In Fig. 2 we present the polymerization rate–time profiles of both activation methods for comparison.

We also used TEA instead of TIBA and measured the polymerization rate–time profile (Fig. 3). In comparison with TIBA activation, the maximum rate appears much faster, but it is seven times less active. After reaching the maximum very quickly, the polymerization rate declines rapidly until almost no consumption of propylene is registered.

$$LFeCl_2 \;+\; (Ph_3C)[B(C_6F_5)_4] \;\longrightarrow\; Ph_3CCl \;+\; LF\overset{+}{e}Cl \;\; B(C_6F_5)_4^-$$
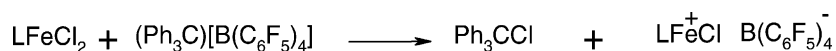
Scheme 1. Reaction of the iron complex with borate.

$$LF\overset{+}{e}Cl \;\; B(C_6F_5)_4^- \;+\; Al\,(iso\text{-}Bu)_3 \;\longrightarrow\; LF\overset{+}{e}\,iso\text{-}Bu \;\; ^-B(C_6F_5)_4 \;+\; Al\,(iso\text{-}Bu)_2Cl$$
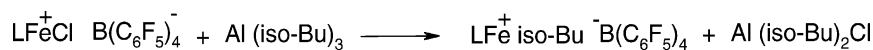
Scheme 2. Reaction of the cationic iron species with TIBA.
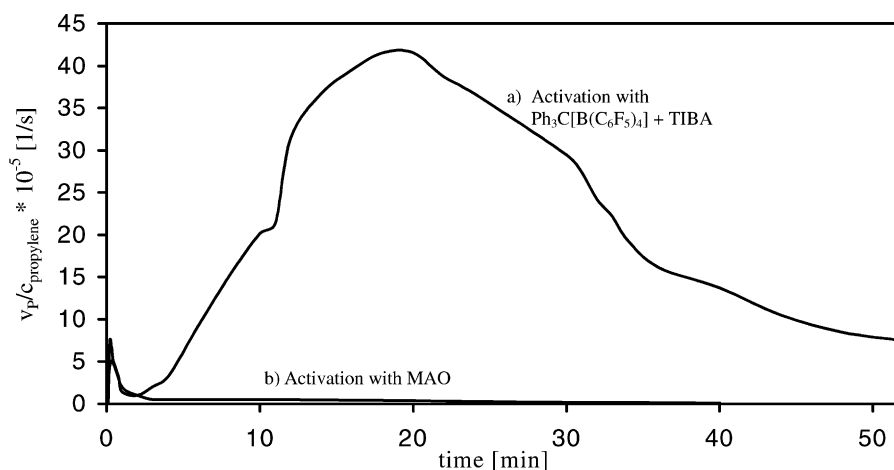
Fig. 2. Polymerization rate–time profiles. (a) [Fe] $= 2.45 \times 10^{-5}$ mol; Ph$_3$C [B(C$_6$F$_5$)$_4$] $= 2.42 \times 10^{-5}$ mol; $p = 1.9$ bar propylene; 0.5 ml TIBA; TP $= 25\,^{\circ}$C; solvent: toluene. (b) [Fe] $= 2.6 \times 10^{-5}$ mol; co-catalyst: MAO 80:1; $p = 1.9$ bar propylene; TP $= 25\,^{\circ}$C; solvent: toluene.
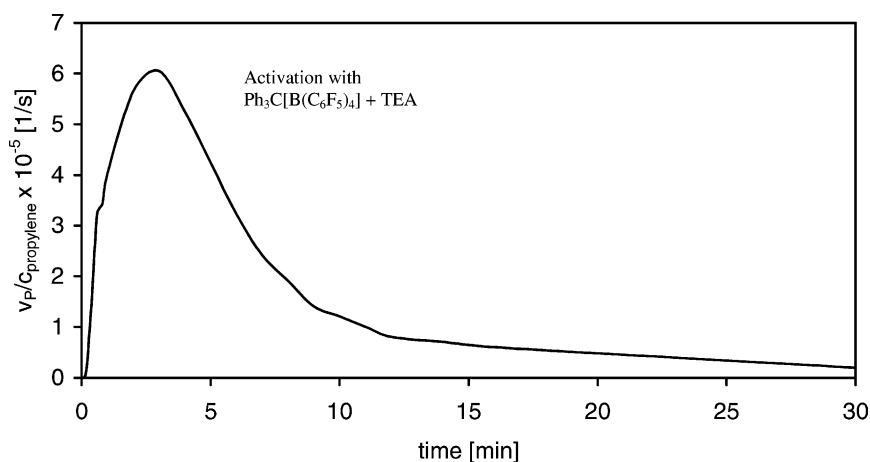

Fig. 3. Polymerization rate–time profile: [Fe] $= 2.45 \times 10^{-5}$ mol; Ph$_3$C [B(C$_6$F$_5$)$_4$] $= 2.42 \times 10^{-5}$ mol; $p = 1.9$ bar propylene; 0.5 ml TEA; TP $= 15\,^{\circ}$C; solvent: toluene.

Table 3
Iron species and polymer endgroups that occur with TIBA and TEA activation

3.3. Endgroup determination

Small and Brookhart [5] investigated this in an earlier work with activation with MMAO. The low molecular weights (∼3500) and high solubilities of the polymer enabled detection of aliphatic endgroups by ^{13}C NMR due to good resolution and high intensity of the signals. The iron species and structures of polymer endgroups are presented in Table 3.

Using TIBA leads to two different aliphatic endgroups. We found both *n*-butyl endgroups and 3-methyl-*n*-butyl endgroups. This shows that propylene is inserted into two different iron alkyl species.

In the case of TEA we found only one aliphatic endgroup: the *n*-propyl endgroup. Small and Brookhart [5] assumed without experimental proof that the *n*-butyl endgroup can only be generated when starting with an iron hydride bond in which propylene inserts via a 1,2 mechanism to form an iron *n*-propyl species. Subsequent 2,1 propylene insertion into the iron *n*-propyl species forms the *n*-butyl endgroup in the polymer. In this report we will demonstrate the experimental evidence for the suggested iron hydride species and show that it plays an important role in the catalytic cycle. The 3-methyl-*n*-butyl endgroup is explained by Brookhart et al. by a 2,1 propylene insertion into an iron isobutyl species, which is formed by activating the iron complex with MMAO (modified MAO, contains 25% isobutyl groups on aluminium).

For clarity we generated different iron alkyls in situ to obtain defined starting species for the propylene polymerization. Corresponding to the second activation step (Scheme 2), only iron isobutyl species exist as the starting species after activation with TIBA. With a subsequent 2,1 propylene insertion the 3-methyl-*n*-butyl endgroup is generated. The termination step via the β-H elimination leads to the iron hydride. To generate the *n*-butyl endgroup it is necessary to start with the iron hydride. Propylene adds to the iron hydride bond via a 1,2 insertion step forming iron *n*-propyl species. Now propylene inserts via a 2,1 step into the previously formed iron *n*-propyl species and generates the *n*-butyl endgroup in the growing polymer.

The same sequence of reaction steps should be observed using TEA in the second activation step. Only iron ethyl groups exist after the second activation step. Via a 2,1 propylene insertion into the iron ethyl bond the *n*-propyl endgroup in the growing polymer is generated. After the β-H elimination step the iron hydride is formed and inserts propylene via a 1,2 mechanism to generate the known iron *n*-propyl bond. This bond is expected to insert propylene via a 2,1 mechanism to generate *n*-butyl endgroups in the growing polymer as is described with TIBA activation. However, only *n*-propyl endgroups are found in the polymer. In the case of TEA there must be a reaction that excludes the iron *n*-propyl species from the 2,1 propylene insertion step. There is only one
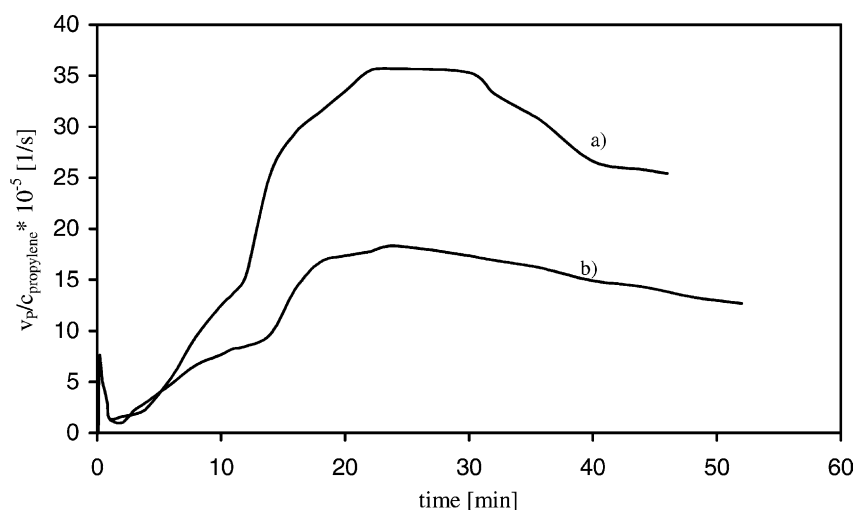
Fig. 4. Polymerization rate–time profiles: (a) polymerization with hydrogen; (b) polymerization without hydrogen. [Fe] $= 2.1 \times 10^{-5}$ mol; Ph$_3$C [B(C$_6$F$_5$)$_4$] $= 2.05 \times 10^{-5}$ mol; $p = 1.9$ bar propylene; 0.1 ml TIBA; TP $= 16\,^{\circ}$C; solvent: toluene.

plausible explanation: the iron *n*-propyl species is rapidly transformed by exchange with TEA into an iron ethyl bond which generates the *n*-propyl endgroup in the polymer after a 2,1 propylene insertion step.

3.4. Influence of hydrogen on the polymerization[16]

The previous discussion provides further evidence for the statement, that an iron hydride species is a central part in the catalytic cycle of propylene polymerization. In Fig. 4 and Table 4 we show the influence of hydrogen on the polymerization rate–time profiles. Adding 8 vol.% hydrogen to the polymerization as described in Section 2 leads to an almost 100% increased activity.

This implies that addition of hydrogen must lead to a higher concentration of active species. In Scheme 3 the reaction that generates the more active iron hydride is shown.

The iron isobutyl species, formed in the second activation step, reacts with added hydrogen to generate the highly active iron hydride. The polypropylene products from reactions containing hydrogen were analysed by ^{13}C NMR spectroscopy. As seen in the spectrum (Fig. 5), only the *n*-butyl endgroup can be detected in the polymer. Although TIBA was used for the second activation step no 3-methyl-*n*-butyl groups can be detected in the polymer obtained.

Scheme 3 implies that all iron isobutyl species are transformed into iron hydride species, because the characteristic 3-methyl-*n*-butyl endgroup for 2,1 propylene insertion in the iron isobutyl bond is not detectable. As an effect of hydrogen addition the molecular mass goes down to 1300 and the $M_{\mathrm{w}}/M_{\mathrm{n}}$ value rises up slightly to 1.8. The reason for the
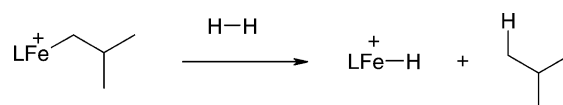
Scheme 3. Reaction of the iron isobutyl species with hydrogen generating a high active species for propylene polymerization.

Table 4

Comparison of polymerizations without and with hydrogen 16 °C (solvent: toluene)

Conditions	FeLCl$_2$ (mol/l)	Ph$_3$C [B(C$_6$F$_5$)$_4$] (mol/l)	TIBA (ml)	Max. activity (1/s mol[C$_3$H$_6$])	Yield (g)	M_{n}	$M_{\mathrm{w}}/M_{\mathrm{n}}$
Without H$_2$	2.1×10^{-5}	2.05×10^{-5}	0.1	1.8×10^{-4}	3.68	3500	1.40
With H$_2$	2.1×10^{-5}	2.05×10^{-5}	0.1	3.6×10^{-4}	6.76	2000	1.80
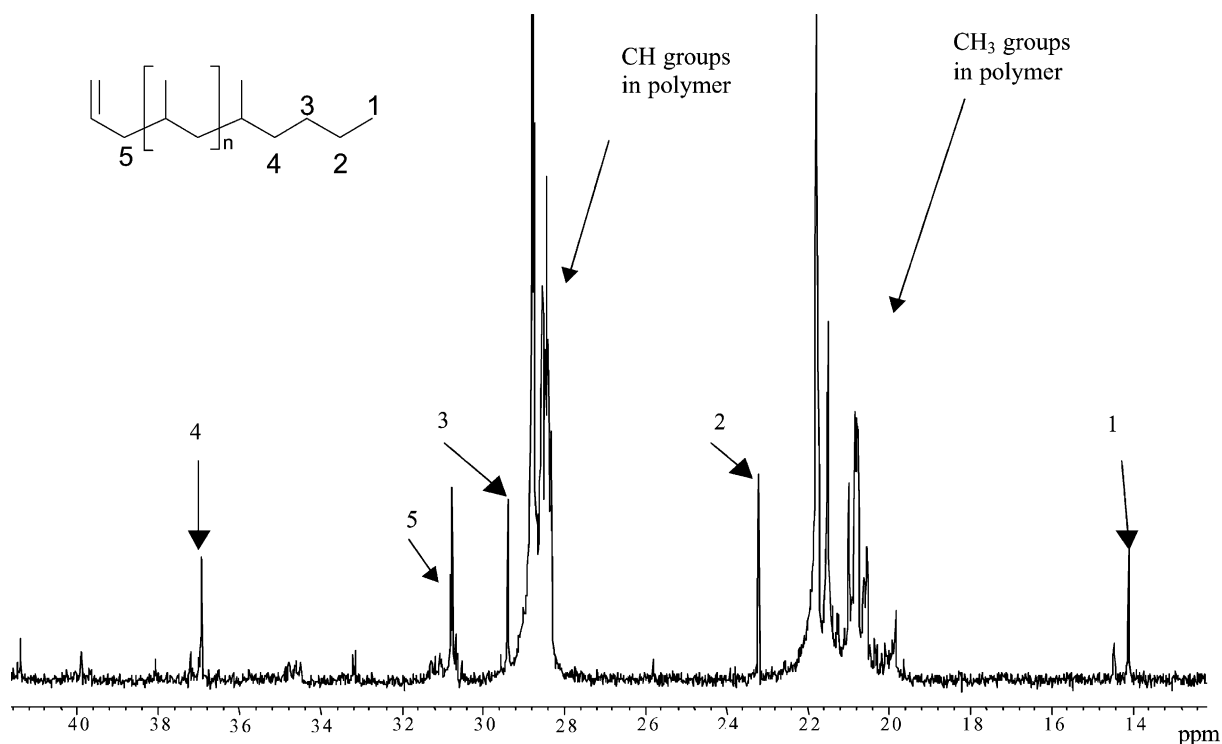
Fig. 5. ^{13}C NMR spectrum of a polypropylene made with hydrogen addition conditions: [Fe] = Ph$_3$C [B(C$_6$F$_5$)$_4$] = 2.5×10^{-5} mol; $p = 1.9$ bar propylene; TP = 5 °C; 0.5 ml TIBA; solvent: toluene; 8 vol.% hydrogen.

lower molecular mass is, according to the reaction in Scheme 3, the reaction of hydrogen with the growing polymer chain. This yields a new iron hydride species and the chain reaction can continue.
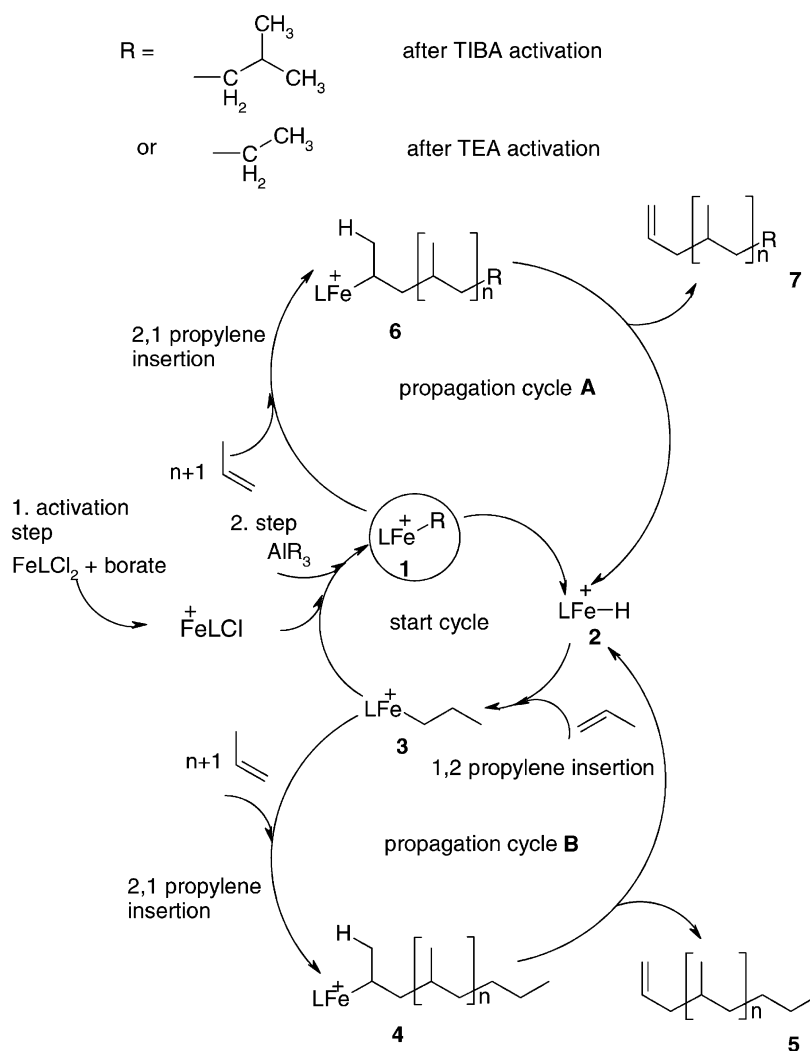
3.5. Catalytic cycle

With the knowledge of the polymer endgroup formation and consideration of the experimentally proven iron hydride species we can formulate for the first time the complete catalytic reaction cycle in Scheme 4 and upgrade the earlier published cycle from Small and Brookhart [5].

It might be helpful to have a look back at Table 4, where all occurred iron alkyl species and polymer endgroups are mentioned. In the polypropylenes made by the TIBA activation we found 45% 3-methyl-*n*-butyl endgroups and 55% *n*-butyl endgroups. Due to this product distribution we can say that chain propagation cycles A and B contribute about 50% to the polymer growth in each case.

From the iron *n*-propyl species **3**, the reaction can follow two different competing courses. Through realkylation with TIBA the iron isobutyl species **1** can be generated, which continuously inserts propylene in a 2,1 step to form species **6** in propagation cycle A. On the other hand 2,1 propylene insertion in species **3** in propagation cycle B leads to species **4**. Hence, realkylation and 2,1 propylene insertion are running in competition. After β-H elimination from a grown polymer species **4** or **6** the iron hydride **2** is generated and the polymers **5** and **7** are formed. The very active iron hydride **2** inserts propylene in a unique 1,2 step to form the iron *n*-propyl species **3** and the catalytic cycle is closed.

With regards to the 55 to 45% polymer endgroup ratio we studied the influence of the TIBA concentration. Under the polymerization conditions described in Section 2 the propylene concentration is 130 times higher than the TIBA concentration in toluene. Despite the great excess of propylene, the 2,1 propylene insertion and the realkylation have the same rates,

Scheme 4. Catalytic cycle for start, chain growth and chain termination for propylene polymerization with bisiminepyridine iron complexes and the described activation.

indicated by the polymer endgroup ratio of almost 50–50. Consequently the realkylation from the iron *n*-propyl species **3** to the iron isobutyl species **1** is about 130 times faster than the 2,1 propylene insertion into the iron *n*-propyl bond. Reducing the TIBA amount to 0.1 ml the propylene concentration is now 650 times higher and amount of the 3-methyl-*n*-butyl endgroups in the polymer declines from 45 to 10%. Because of lower TIBA concentration the realkylation is decreased and propagation cycle B is favoured. It is of course conceivable that the growing chain

species **4** and **6** could be realkylated as well as species **3**, but this does not take place because these species are secondary iron alkyls. The steric bulkiness prevents realkylation of species **4** and **6**. Addition of hydrogen to the reaction containing TIBA yields a polymer with *n*-butyl endgroups (species **5**). According to Scheme 3 the iron isobutyl species is transformed by hydrogen to an iron hydride. In Scheme 4 this reaction is the step from species **1** to **2**. In this case we only run through propagation cycle B.

Using TEA instead of TIBA leads only to *n*-propyl endgroups in the polymer. These groups are formed by 2,1 propylene insertion into an iron ethyl species. According to Scheme 4 it means that we only run through propagation cycle A.

We showed that if the realkylation is faster and more complete, the smaller is the alkyl of the aluminiumtrialkyl. The isobutyl group in TIBA is bigger than the *n*-propyl in species **3** and cannot substitute it completely. So there are still iron *n*-propyl bonds in which propylene can insert and generate the *n*-butyl endgroups in the polymer. With pure TIBA activation we run through propagation cycle A and B, but using TEA gives rise to a different situation. The ethyl group in TEA is smaller than the *n*-propyl group in species **3** and substitutes it completely to form an iron ethyl bond which leads to *n*-propyl aliphatic endgroups in the polymer.

4. Conclusion

Activating 2,6-bis [1-(2-isopropy-6-methylphenyl-imino)ethyl]-pyridineiron(II)dichloride with Ph$_3$C [B(C$_6$F$_5$)$_4$] and subsequent treatment with TIBA generates highly active catalysts for propylene polymerization. The activity is much higher than that obtained with MAO and even higher than using MMAO. Detection of the propylene consumption with mass-flowmeters allows the first view of the kinetic profile of propylene polymerization with this type of catalysts. We assume an iron hydride species to be a key species in the catalytic cycle, because the detected aliphatic endgroups in the polypropylenes can only be explained when an iron hydride is involved.

Increased activity on addition of hydrogen to the reaction mixture confirms the presence of the highly active iron hydride in the catalytic cycle (Scheme 4). Using different aluminiumtrialkyls (TIBA, TEA) and varying their amount in the polymerization allows control of the mechanism in the propagation cycle.

References

[1] L.K. Johnson, C.M. Killian, M. Brookhart, J. Am. Chem. Soc. 117 (1995) 6414–6415.
[2] M. Brookhart, et al., Macromolecules 33 (2000) 2320–2334.
[3] B.L. Small, M. Brookhart, J. Am. Chem. Soc. 120 (1998) 7143–7144.
[4] B.L. Small, M. Brookhart, A.M.A. Bennett, J. Am. Chem. Soc. 120 (1998) 4049–4050.
[5] B.L. Small, M. Brookhart, Macromolecules 32 (1999) 2120–2130.
[6] K. Yang, R.J. Lachicotte, R. Eisenberg, Organometallics 17 (1998) 5102–5113.
[7] G.J.P. Britovsek, V.C. Gibson, B.S. Kimberley, P.J. Maddox, S.J. McTavish, G.A. Solan, A.J.P. White, D.J. Williams, Chem. Commun. (1998) 849.
[8] V.C. Gibson, et al., J. Am. Chem. Soc. 121 (1999) 8728–8740.
[9] G.J.P. Britovsek, V.C. Gibson, D.F. Wass, Angew. Chem. 111 (1999) 448–468.
[10] A.M.A. Bennett (invs.), E.I. Du Pont de Nemours and Company, WO 98/27124, 1998.
[11] M.S. Brookhart, B.L. Small (invs.), WO 98/30612, E.I. Du Pont de Nemours and Company, 1998.
[12] A.M.A. Bennett, Chemtech (1999) 24–28.
[13] European Chemical News, July 30–August 5, 2001, pp. 20–21.
[14] E.P. Talzi, D.E. Babushkin, N.V. Semikolenova, V.N. Zudin, V.A. Zakharov, Kinetics, Kinet. Catal. 42 (2) (2001) 147–153.
[15] V.C. Gibson, et al., J. Chem. Soc., Dalton Trans. (2002) 1159–1171.
[16] T. Hayashi, Y. Inoue, R. Chujo, T. Asakura, Macromolecules 21 (9) (1988) 2675–2684.